

Supramolecular Chemistry



ISSN: (Print) (Online) Journal homepage: www.tandfonline.com/journals/gsch20

The suprachelate effect: a pathway to supramolecules with Cu(II) and ethylenediamine

Fenton C. Lawler, Ryan S. Storteboom, Plinio D. Rosales-Lopez, Katherine J. Selvaggio, Krista A. Zogg, Trevina Chen, Dafna L. Heule, Madison N. Hoogstra, Orin R. Daspit, Magdalene A. Grabill, Adelaide A. Stonehouse, Anna E. Jipping, Aerin E. Baker & Douglas A. Vander Griend

To cite this article: Fenton C. Lawler, Ryan S. Storteboom, Plinio D. Rosales-Lopez, Katherine J. Selvaggio, Krista A. Zogg, Trevina Chen, Dafna L. Heule, Madison N. Hoogstra, Orin R. Daspit, Magdalene A. Grabill, Adelaide A. Stonehouse, Anna E. Jipping, Aerin E. Baker & Douglas A. Vander Griend (10 Oct 2024): The suprachelate effect: a pathway to supramolecules with Cu(II) and ethylenediamine, Supramolecular Chemistry, DOI: 10.1080/10610278.2024.2410768

To link to this article: https://doi.org/10.1080/10610278.2024.2410768

+	View supplementary material 🗷
	Published online: 10 Oct 2024.
	Submit your article to this journal 🗷
Q ^L	View related articles 🗷
CrossMark	View Crossmark data 🗗





The suprachelate effect: a pathway to supramolecules with Cu(II) and ethylenediamine

Fenton C. Lawler, Ryan S. Storteboom, Plinio D. Rosales-Lopez, Katherine J. Selvaggio, Krista A. Zogg, Trevina Chen, Dafna L. Heule, Madison N. Hoogstra, Orin R. Daspit, Magdalene A. Grabill, Adelaide A. Stonehouse, Anna E. Jipping, Aerin E. Baker and Douglas A. Vander Griend

Department of Chemistry and Biochemistry, Calvin University, Grand Rapids, MI, USA

ABSTRACT

This paper portrays the solution-phase dynamics as copper(II) and ethylenediamine explore a multitude of different complexes. The data from five spectrophotometric titrations were globally analysed, evidencing four predominant species ($[Cu]^{2+}$, $[Cu(en-N,N')]^{2+}$, $[Cu(en-N,N')_2]^{2+}$, $[Cu(en-N,N')_2]^{2+}$, $[Cu(en-N,N')_2]^{2+}$, along with their molar absorptivity curves and associative binding constants. The data also seem to support a fifth species, $[Cu_2(\mu-en-N,N')]^{4+}$, in which ethylenediamine bridges two Cu(II) centres. The thermodynamic stability of all five species is corroborated by *ab initio* computational calculations. The potential existence of $[Cu(en-N)_4]^{2+}$ highlights the suprachelate effect – going beyond the chelate effect – where multidenticity is overtaken by monodenticity. Such dangling multidentate ligands are available to bind to additional metal centres and thus build towards self-assembling supramolecules.



ARTICLE HISTORY

Received 27 June 2024 Accepted 23 September 2024

KEYWORDS

Supramolecular; chelate; suprachelate; spectroscopic titration; global analysis

Introduction

When textbooks introduce the chelate effect, copper(II) and ethylenediamine (en) are often the featured example [1]. This well-known chemistry explains 'the unusual stability of a coordination compound involving a chelating, multidentate ligand as compared to equivalent compounds involving monodentate ligands' [2]. Copper(II), with its four primary coordination sites, readily binds four monodentate or two bidentate ligands in a square planar fashion [3]. Entropy drives the release of the monodentate ligands into the solution in favour of the bidentate ligands in the primary coordination sphere [4].

It is the solution phase in which metal cations and ligands explore many possible configurations and

assemble into supramolecules. En, for example, could chelate, bridge, or dangle. Ethylenediamine has been found to bridge Ni(II) in solution [5], as well as bridge Cu(II) [6], Ni(II) [7], Mn(II) [8], Cd(II) [9], and Ru(II) [10]. characterised in the solid state.

In solution, it appears that Cu(II) will coordinate with more than two ethylenediamine ligands only if the solvent is greater than 10% en [11]. Sharma *et al.* take advantage of this fact to crystallise the first pentacoordinate Cu(II)/en complex, which has a monodentate, dangling en. Both the crystals and supernatant were blue. The colour of Cu(II) solutions is indicative of the number of amine ligands in the primary coordination sphere. With four amine ligands, the aqueous solution will be purple with an absorbance maximum at 548 nm.

With more amine ligands, the colour shifts back to an absorbance maximum around 605 nm, appearing blue [12]. This is known as the pentaamine effect [13]. Chattopadhyay et al. confirm that copper(II) resists using coordination sites beyond four, as a second tridentate ligand dangles rather than adopting octahedral coordination around the metal centre [14].

Further establishing the existence of monodentate en, Inada et al. used nitrogen-14 NMR, XAFS, and spectroscopy to capture the dynamic exchange for the Cu(II)/en system in solution. They found that the ethylenediamine ligands exchange rapidly through an associative mechanism that involves multiple dangling ethylenediamine for the transition states. Wang et al. find that ethylenediamine adopts several different low energy arrangements around Cu(II): bidentate, monodentate, and an intramolecular H-bond ring in which the non-coordinated amine H-bonds to the coordinated one.

Characterising complicated homogeneous systems such as aqueous Cu(II)/en requires a specialised tool like Parametric Equilibrium Restricted Global Analysis [15,16]. UVvis measurements on a series of sequential chemical solutions can be modelled to identify all distinct chemical species present, their molar absorptivity curves, and the associative binding constants for the reactions between them [17-19]. The dynamics of any equilibrated system can be captured no matter what arrangements the metal and ligands adopt.

As introduced above, the chelate effect drives bidentate ligands like ethylenediamine to substitute for monodentate ligands, like ammonia or ethyl amine. But what happens when excess ethylenediamine is available? Numerous examples where ethylenediamine uses only one nitrogen atom to bind to the cationic centre are energetically feasible [20]. If the entropy of a dangling ethylenediamine is sufficiently high, it would seem likely that a complex with dangling ethylenediamines might be entropically favoured. If additional H-bonds form, the complex might be enthalpically favoured. In this work, we present how monodenticity overtakes multidenticity, favouring dangling multidentate ligands. We designate this as the suprachelate effect. This is exemplified by the species [Cu(en-N)₄]²⁺, with four dangling ethylenediamine ligands, as detailed below.

Methodology

Reagents

 $Cu(NO_3)_2 \cdot 3 h_2O$ (Sigma-Aldrich, 99.5 wt%), $Cu(CIO_4)_2 \cdot$ 6 h₂O (Sigma-Aldrich, 98 wt%), and ethylenediamine (Sigma-Aldrich, ≥99 wt%) ligand were used as purchased. Warning: perchlorate salts are potentially explosive [21].

Preparation of solutions

Each analyte solution was made as follows. Approximately, 0.1 g (0.0004 mol) of $Cu(NO_3)_2 \cdot 3 h_2O$ or 0.2 g (0.0005 mol) $Cu(ClO_4)_2 \cdot 6 H_2O$ was dissolved in deionised water in a 50 mL volumetric flask to create a ~0.01 M solution.

Each titrant solution was made as follows. Approximately, 0.1 mL ethylenediamine along with 0.06 g (0.0002 mol) of $Cu(NO_3)_2 \cdot 3 H_2O$ or 0.09 g (0.0002 mol) $Cu(ClO_4)_2 \cdot 6H_2O$ was dissolved in deionised water in a 25 mL volumetric flask to create a ~0.1 M solution.

Details for all five titration experiments can be found in Table 1.

Titrations

Five spectrophotometric titrations were performed by titrating a solution of ethylenediamine and Cu(II) into a solution of Cu(II).

DS1 was collected with a custom autotitrator adapted from an Olis design that powers two syringes, one of which injects titrant into the cuvette from the top and the other that circulates analyte solution from the bottom of the cuvette to mix in between scans. Twenty-five microlitres of titrant solution were added at a time to ~4 mL of the analyte solution. This enabled the titration to proceed overnight and allowed for longer equilibration times between additions.

DS2-5 were collected manually, incrementally adding 10-20 µL of titrant solution using micro-syringes to a starting analyte volume of 1.5 mL (DS2-3) or 2 mL (DS4-5). After two equivalents, the titrant solution volume was increased to 50–100 μL. Magnetic stir bars were included in each cuvette to aid mixing.

Table 1. The precise concentrations and experimental details for the five spectrophotometric datasets.

Data		Cu(II) conc.		Eq. of		Data range		
set	Analyte	(M)	en conc. (M)	en	Number of solutions	(nm)	Temp. (K)	Spectrometer model
DS1	Cu(ClO ₄) ₂	0.0103	0.156	5.18	82	400-850	298	Olis 14
DS2	$Cu(NO_3)_2$	0.0099	0.08	4.25	58	400-850	295	Hitachi U-3900H
DS3	$Cu(NO_3)_2$	0.0099	0.08	4.02	45	400-900	295	Varian Cary 50Bio
DS4	$Cu(NO_3)_2$	0.01115	0.08	4.30	89	400-900	296	Varian Cary 50Bio
DS5	$Cu(ClO_4)_2$	0.01003	0.08	4.06	61	400-850	295	Hitachi U-3900H

Spectrophotometry

Three different spectrometers were used to collect the data: an OLIS 14 UV/VIS/NIR, a Hitachi U-3900 h, and a Varian Cary (Table 1). All data were collected around 296 K relative to a baseline of deionised water. DS1 was collected using quartz cuvettes, and DS2–5 were collected using plastic cuvettes. The OLIS spectrophotometer was set to 10 reads per datum, while the Hitachi and Cary were set to one read per datum. Absorbance scans were taken after each addition of the titrant.

Chemometric modeling

All titration data were analysed using *Sivvu.org* to perform Parametric Equilibrium Restricted Global Analysis (PERGA), which models spectrophotometric titration data according to various sets of chemical species and their associated binding reactions [16].

First, the number of additive mathematical factors that exist within the data can be determined through singular value decomposition (SVD) [22]. Each significant factor corresponds to a distinct chemical species. From this, models consisting of lists of chemical species in equilibrium with each other are fit against the data to optimise the stepwise associative binding constants. *Sivvu.org* then calculates molar absorptivity curves for each distinct chemical species. A model is determined to fit the data well when the molar absorptivity curves are chemically reasonable, while the root mean square residuals (RMSR) are minimised. *Sivvu.org* also calculates the 95% confidence intervals on the logK values using bootstrapping – done 100 times for all proposed models [23].

Computational modeling

All computational calculations were performed using Gaussian 16 with the WebMO user interface. Cu(II) ethylenediamine complexes were optimised using density functional theory (DFT) with the Becke, 3-parameter, Lee–Yang–Parr (B3LYP) functional method and GEN keyword with LANL2DZ (Los Alamos National Lab 2 Double ζ) for Cu(II) and cc-pVTZ for the rest of the atom basis sets. Proper geometry was ensured by using a Comprehensive – Mechanics cleanup, and all species were modelled in a water solvent field. Besides total energy values, thermodynamic quantities (free energy, enthalpy, and entropy) were then obtained using vibrational frequency calculations.

Results

Each of the five spectrophotometric titrations yielded coherent absorbance data over at least four equivalents of en. Figure 1 shows raw absorbance spectra for DS1.

Significant factors

SVD was performed on each of the datasets to determine the number of significant contributing mathematical factors (Table 2). Factors are considered significant if their weight is at least double that of the following factor. Factors might be significant if their weight is at least 10% greater than the following factor, indicating an absorbing chemical species that may be present. Any factor that is not 10% greater than the following factor is insignificant and can be attributed to random noise.

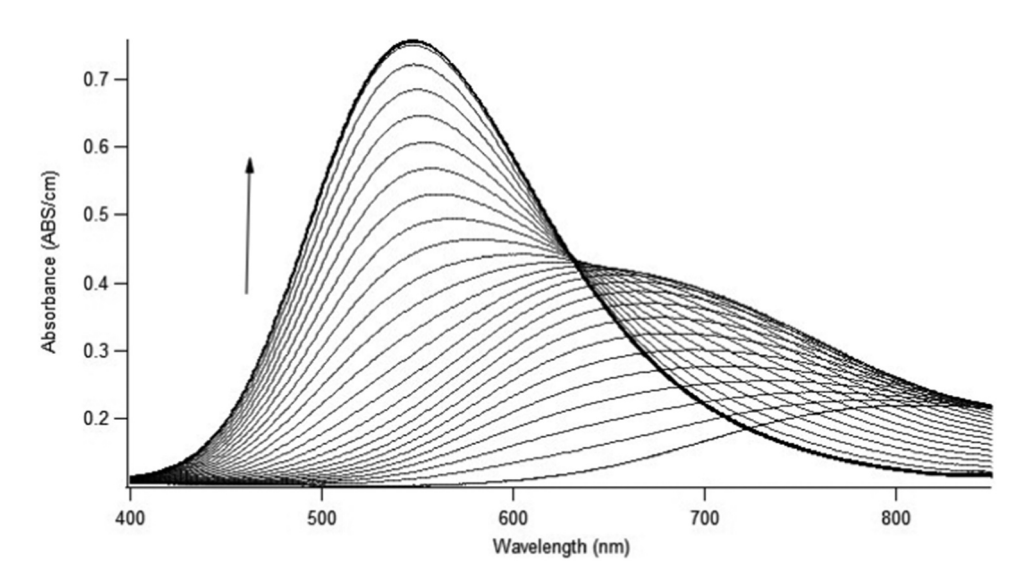


Figure 1. DS1 absorbance spectra. 82 solutions of aqueous 0.0103 M $Cu(CIO_4)_2$ titrated with 0.156 M ethylenediamine from 0 to 5.18 equivalents. Data is upshifted by 0.1 ABS/cm [19]. All datasets resemble this set of spectra. (see supporting information for additional datasets).

Table 2. The 10 largest SVD weights for each dataset, listed in ranked order. Bolded factors are significant. Factors in regular font are semi-significant. Factors in light gray font are not significant.

Factor	DS1	DS2	DS3	DS4	DS5
1	67.2980	43.8586	32.2782	67.7861	44.8979
2	12.2363	11.4141	10.6123	17.6298	12.8880
3	2.1230	1.9451	1.7684	2.6317	2.1191
4	0.0655	0.0534	0.1143	0.1708	0.1565
5	0.0086	0.0326	0.0194	0.0618	0.0457
6	0.0066	0.0296	0.0153	0.0461	0.0414
7	0.0050	0.0260	0.0121	0.0317	0.0383
8	0.0049	0.0205	0.0105	0.0306	0.0235
9	0.0049	0.0171	0.0088	0.0264	0.0222
10	0.0048	0.0165	0.0065	0.0252	0.0208

Four of the five datasets indicate at least four significant factors, and all datasets indicate at least six factors which are possibly significant. Based on SVD analysis and conventional understanding of the Cu(II)/en system, three-factor, four-factor and five-factor models were proposed and tested. Literature supports the following three species as part of the model: [Cu]²⁺, [Cu(en-N, $(N')^{2+}$, $[Cu(en-N,N')_2]^{2+}$. These species comprise the three-factor model, which fit the data well but left significant features in the data unaccounted for. These three were subsequently used as a basis for the four and five-factor models.

Four-factor model

Datasets were fitted to various four-factor models in Sivvu.org, many of which consistently resulted in low RMSR values (Table 3) and chemically reasonable molar absorptivity curves (Figure 2).

Because the RMSR values are generally lower, the fourth species appears to be a monometallic complex $([Cu(en-N)_n]^{2+} n = 3-6)$ and not ethylenediamine itself or a bimetallic bridging species like $[Cu(\mu-en-N,N')]^{4+}$. Differentiating on the number of ethylenediamine groups around a Cu(II) centre is less conclusive on the basis of RMSR because regardless of whether n is 3, 4, 5, or 6, the concentration curves of each would start to grow in at the same point during the course of the titration and increase through the end of the titration. This makes it difficult to distinguish them from each other with PERGA. Therefore, we turn to the molar absorptivity curves to resolve the number of ethylenediamine ligands in the fourth species (Figure 2).

Whether the number of ethylenediamine ligands is modelled as four, five, or six, the molar absorptivity curve for the fourth species candidates, $[Cu(en-N)_n]^{2+}$, presents a maximum around 548 nm, identical to that of [Cu(en- $N.N^3$ ₂1²⁺. This indicates that the number of amine groups coordinated to the Cu(II) is four. This eliminates the possibility of n = 5 or n = 6 because these species

Table 3. RMSR values for various four-factor models in which the first three species are $[Cu]^{2+}$, $[Cu(en-N,N')]^{2+}$, $[Cu(en-N.N)_{2}]^{2+}$ and the fourth species is listed in column 1

[Ca(Cii 14,14 /2]	una the	louren species is	iistea iii eolaliiii i	•		
Fourth species		DS1	DS2	DS3	DS4	DS5
[Cu(en-N) ₂ (en-N,	N')] ²⁺	0.001354	0.002196	0.002079	0.002377	0.001485
$[Cu(en-N)_4]^{2+}$		0.000961	0.001879	0.001713	0.002092	0.001419
[Cu(en-N) ₅] ²⁺		0.000757	0.00161	0.001534	0.001727	0.001343
[Cu(en-N) ₆] ²⁺		0.000723	0.001486	0.001463	0.001568	0.001307
[Cu ₂ (μ-en-N,N')] ⁴	+	0.001727	0.002057	0.002494	0.002394	0.002663
en		0.000981	0.002186	0.002108	0.002452	0.001485

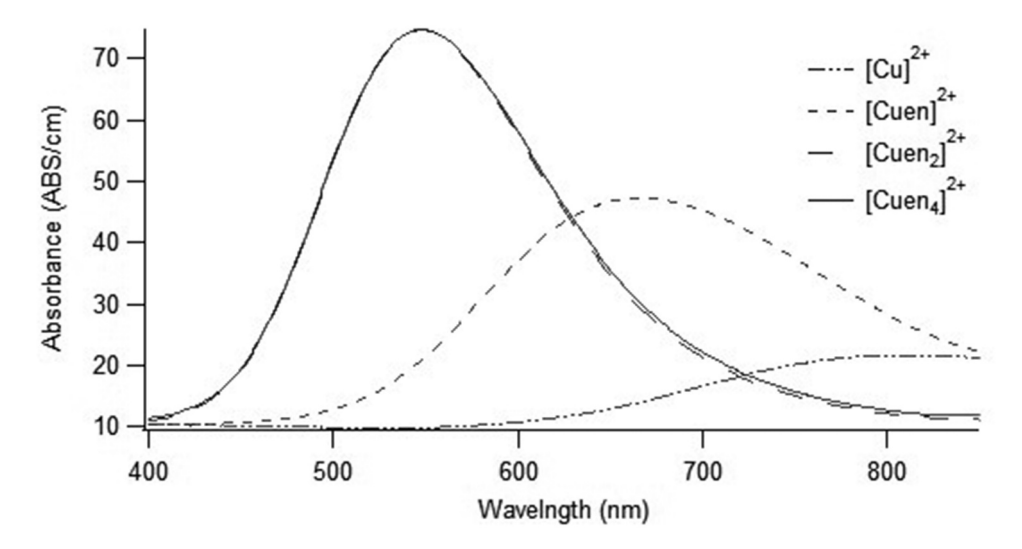


Figure 2. Molar absorptivity curves for the four-factor model fit to DS1.

Table 4. RMSR (restricted and unrestricted) for DS1–5 when fitted to the proposed four-factor model. The Δ signifies the difference between restricted and unrestricted RMSRs. The $\Delta\Delta$ values signify the difference between the two Δ values and indicate the plausibility of the fourth factor.

Dataset	3-factor restricted RMSR	3-factor unrestricted RMSR	3-factor RMSR Δ	4-factor restricted RMSR	4-factor unrestricted RMSR	4-factor RMSR Δ	ΔΔ
DS1	0.00194	0.00040	0.00154	0.00096	0.00018	0.00078	0.00076
DS2	0.00251	0.00087	0.00164	0.00188	0.00078	0.00110	0.00053
DS3	0.00272	0.00080	0.00192	0.00171	0.00027	0.00144	0.00048
DS4	0.00283	0.00084	0.00199	0.00209	0.00048	0.00161	0.00038
DS5	0.00289	0.00127	0.00143	0.00142	0.00082	0.00060	0.00083

necessarily have more than four amines coordinated, and if more than four amines are coordinated, the molar absorptivity maximum is expected to redshift because of the pentaamine effect [13]. For all five datasets, the maximum absorbance exclusively blueshifts throughout the entire titration. The absence of any redshifting indicates that there is never a fifth amine that binds to the copper(II) centre.

Both $[Cu(en-N)_2(en-N,N')]^{2+}$ and $[Cu(en-N)_4]^{2+}$ could exist as a pseudo-square planar complex with four amines coordinated. [Cu(en-N)₂(en-N,N')]²⁺ would have two ethylenediamine ligands that dangle, while the other one binds conventionally through both nitrogen atoms. $[Cu(en-N)_4]^{2+}$ would have four ethylenediamine ligands that dangle with only one of their two amine groups coordinated to the central copper ion. The RMSR values are lower for the latter in all but one dataset. Furthermore, for DS5, the resulting molar absorptivity curve for $[Cu(en-N)_2(en-N,N')]^{2+}$ is nonsensical. In reality, both species may exist in solution together, but this type of analysis would not resolve them well, so a single representative species works best in the model. Therefore, $[Cu(en-N)_{4}]^{2+}$ serves as the best representative species.

Adding $[Cu(en-N)_4]$ [2]. as the fourth factor lowers the RMSR values (Tables 3 and 4), both restricted and unrestricted, as expected when adding any additional species to a model. The unrestricted RMSR is the mathematical error of the fit, which is necessarily lower than the restricted RMSR - the error of the chemically restricted fit. However, a merited chemical species will lower the restricted RMSR value more than it lowers the unrestricted RMSR value. The Δ values in Table 4 correspond to the difference between the restricted and unrestricted RMSR values. The $\Delta\Delta$ values correspond to the difference between the Δ values, and they represent how much the four-factor models decrease the residual error gap, thus establishing the legitimacy of [Cu(en-N)₄]²⁺ as the fourth chemical species.

The molar absorptivity curves for the four species vary only slightly from one dataset to the next (see Supporting Information for details). Curves from DS1

are shown in Figure 2. The peak shift as ethylenediamine is added fits crystal field theory as amine ligands replace water around the Cu(II), two at a time [1]. The average molar absorptivity peak positions are given in Table 5 and compared to literature values. The molar absorptivity curves for $[Cu(en-N,N')_2]^{2+}$ and $[Cu(en-N)_4]^{2+}$ overlap significantly because they each have four binding sites occupied by amines (Figure 2, Table 5). Despite the similarities in the electronic structures of these two complexes, the differences between the curves point to the presence of two distinct species that show up in separate parts of the titration.

The binding constants for the four-factor model were quantified via PERGA and are shown in Table 6. The refinement for each dataset was started at the same initial logK values (10.5, 9.2, and 5.2) and while some increased and others decreased upon optimisation, the results were very consistent overall.

Since there is no mathematically straightforward way to combine multiple values and their respective confidence intervals [26]. Table 7 presents several options for combining the logK values from the five different titration experiments. First, the simplest way is to average them, calculate a standard deviation, and define the 95% confidence interval as two standard deviations. This incorrectly assumes that the

Table 5. Molar (per copper) absorptivity peak position (nm) followed by peak height with standard deviations for the spectroscopic transitions of the copper(ii) complexes with ethylenediamine in water between 400 and 850 nm as determined by the modelling of five spectrophotometric datasets at 295 K.

Complex	$^{2}T_{2g} \rightarrow ^{2}E_{g}$ (D)	Reference
[Cu] ²⁺	807.8 (14.12 ± 2.76)	*
[Cu] ²⁺	~810 (~10)	[12]
[Cu(en- <i>N,N′</i>)] ²⁺	667.5 (37.64 ± 2.25)	*
[Cu(en- <i>N,N′</i>)] ²⁺	~660 (~35)	[24]
[Cu(en- <i>N,N′</i>)] ²⁺	~660 (~35)	[12]
$[Cu(en-N,N')_2]^{2+}$	548.6 (64.74 ± 1.98)	*
$[Cu(en-N,N')_2]^{2+}$	~545 (~65)	[24]
$[Cu(en-N,N')_2]^{2+}$	~545 (~75)	[25]
$[Cu(en-N,N')_2]^{2+}$	~540 (~60)	[12]
$[Cu(en-N)_4]^{2+}$	548.4 (64.51 ± 2.38)	*
[Cu ₂ (μ-en- <i>N,N</i> ′)] ⁴⁺	701.6 (69.6 ± 25.4)	*

^{*}This work.



Table 6. Binding constants (logK) for the four-factor model with their respective 95% confidence intervals.

Reaction	DS1	DS2	DS3	DS4	DS5
$[Cu]^{2+} + en \Rightarrow [Cu(en-N,N')]^{2+}$	$10.74^{+0.09}_{-0.03}$	$10.24^{+0.07}_{-0.07}$	$10.16^{+0.08}_{-0.10}$	$10.30^{+0.09}_{-0.10}$	10.75 ^{+0.07} _{-0.04}
$[Cu(en-N,N')]^{2+} + en \Rightarrow [Cu(en-N,N')_2]^{2+}$	$9.26^{+0.06}_{-0.03}$	$8.71^{+0.03}_{-0.03}$	$8.66^{+0.06}_{-0.04}$	$8.72^{+0.06}_{-0.04}$	$9.26^{+0.06}_{-0.03}$
$1/_{2}[Cu(en-N,N')_{2}]^{2+} + en \Rightarrow 1/_{2}[Cu(en-N)_{4}]^{2+}$	$6.74^{+0.25}_{-0.33}$	$6.47^{+0.27}_{-0.33}$	$6.43^{+0.32}_{-0.20}$	$6.50^{+0.21}_{-0.31}$	$6.55^{+0.36}_{-0.25}$

The uncertainty ranges for the logK values are quite small. Each dataset seems to support the model tightly, but some of the ranges do not overlap. This is not unexpected when replicate datasets are taken under various experimental conditions and parameters. [5]

Table 7. LogK values for the four-factor model based on all five datasets together. 'Simple Mean' values are the unweighted average of the five logKs from Table 6 with uncertainty ranges of two standard deviations, 'Concatenated datasets' values are generated from fitting all five datasets as a single dataset. 'Common LogKs' values were obtained upon modelling the five datasets simultaneously with the same logK values while allowing the sets of molar absorptivity curves to vary. 'Combined bootstraps' ranges are generated by combining the five bootstrap histograms for each logK and reproducing 95% confidence intervals. 'Best' is the recommended choice, using the mean logKs and the combined bootstraps. Free energy values for the 'best' logK values are also shown in the last column.

Reaction	Simple mean	Concatenated datasets	Common logKs	Combined bootstraps	Best	ΔG° (kJ/mol)
$[Cu]^{2+} + en \Rightarrow [Cu(en-N,N')]^{2+}$	$10.44^{+0.60}_{-0.60}$	$11.96^{+0.55}_{-0.09}$	10.79+8	10.11 – 10.80	$10.44^{+0.36}_{-0.33}$	$-59.6^{+1.9}_{-2.1}$
$[Cu(en-N,N')]^{2+} + en \Rightarrow [Cu(en-N,N')_2]^{2+}$	$8.92^{+0.62}_{-0.62}$	$10.36^{+0.55}_{-0.19}$	9.17^{+8}_{-3}	8.63 - 9.29	$8.92^{+0.37}_{-0.29}$	$-50.9^{+\overline{1.7}}_{-2.1}$
$1/_{2}[Cu(en-N,N')_{2}]^{2+} + en \Rightarrow 1/_{2}[Cu(en-N)_{4}]^{2+}$	$6.54^{+0.24}_{-0.24}$	$3.74^{+2.31}_{-1.64}$	$3.97^{+26}_{-0.4}$	6.21 – 6.90	$6.54^{+0.36}_{-0.33}$	$-37.3^{+\overline{1.9}}_{-2.1}$
RMSR (\times 10 ³)	2.027	160.7	1.982	N/A	2.027	2.027

mathematics of the equilibria is linear and consequently generates symmetric confidence intervals. Another option is to concatenate all five datasets and model as if it were a single dataset. In this case, several datasets needed to be rescaled so that the independent dimension, i.e. the wavelengths, all correspond. Unfortunately, this rarely works for replicate experiments due to their inherent variability [5]. A third option is to model the five datasets simultaneously, forcing them to refine to a single set of logK values while allowing their molar absorptivity curves to vary independently. While this yields the lowest combined RMSR, it requires more involved calculations, and the uncertainty ranges are subject to exergonic launching for larger logK values. Finally, since each dataset has its own bootstrapped histogram of logK values - used to quantify the 95% confidence intervals - a combined histogram can be easily created and used to quantify the 95% confidence interval for all the datasets together. We recommend using the simple means with the combined bootstraps for the uncertainty range.

Our 'Best' logK values match the literature quite well, especially for logK₁. Carlson et al. quantified, using Bjerrum's mathematical method [24], the first two binding events via pH titration at 30°C and $\mu = 0.5$ M KNO₃ $(logK_1 = 10.55; logK_2 = 9.5)$ [27]. Likewise, Basolo and Murmann used pH titration to determine their values at $\mu = 0.5 \text{ M KNO}_3$ and 25°C (logK₁ = 10.76; logK₂ = 9.37) and 0°C ($logK_1 = 11.34$; $logK_2 = 9.95$) [28]. Yogi et al. calculated constants ($logK_1 = 10.32$ and $logK_2 = 8.8$) from pH titration (35°C, $\mu = 0.2 \text{ M KNO}_3$) using nonlinear least-squares [29]. Silva et al. calculated constants $(log K_1 = 10.47 \text{ and } log K_2 = 9.2) \text{ from pH titration } (25^{\circ}\text{C},$

 $\mu = 0.1 \text{ M KNO}_3$) using HYPERQUAD and confirmed with HYSS to determine speciation as a function of pH [30].

Five-factor model

The four-factor model discussed above fits all the datasets sufficiently well. However, the SVD analysis and various smaller remaining features in the residual plots (supporting information), suggest the existence of a fifth factor. Datasets were fit to various five-factor models, in which the first four factors are as above. $[Cu(en-N,N')(en-N)_2]^{2+}$, $[Cu(en-N)_5]^{2+}$, and $[Cu(en-N)_6]^{2+}$ are not viable options as a fifth factor because they did not render sensible molar absorptivity curves. $[Cu_2(\mu-en-N,N')]^{4+}$ did a chemically sensible molar absorptivity curve (Figure 3) and its existence as a bridging species has been suggested by prior work [5]. $[Cu_2(\mu-en-N,N')]^{4+}$ also lowered the restricted RMSR substantially for all five datasets (Table 8) and the positive $\Delta\Delta$ values legitimise it as the fifth chemical species

The logK values for the five-factor model were calculated using PERGA (Table 9).

Table 10, like Table 7, presents the same options for combining the logK values from the five different titration experiments.

The logK values for five-factor model closely match those of the four-factor model as the average of the first two reactions of the five-factor model correlates to the first reaction of the four-factor model. Unexpectedly, the spontaneity of the first reaction, which creates the bridging species and brings together three molecules, surpasses that of the second, which unforms the bridging species and does not impact the

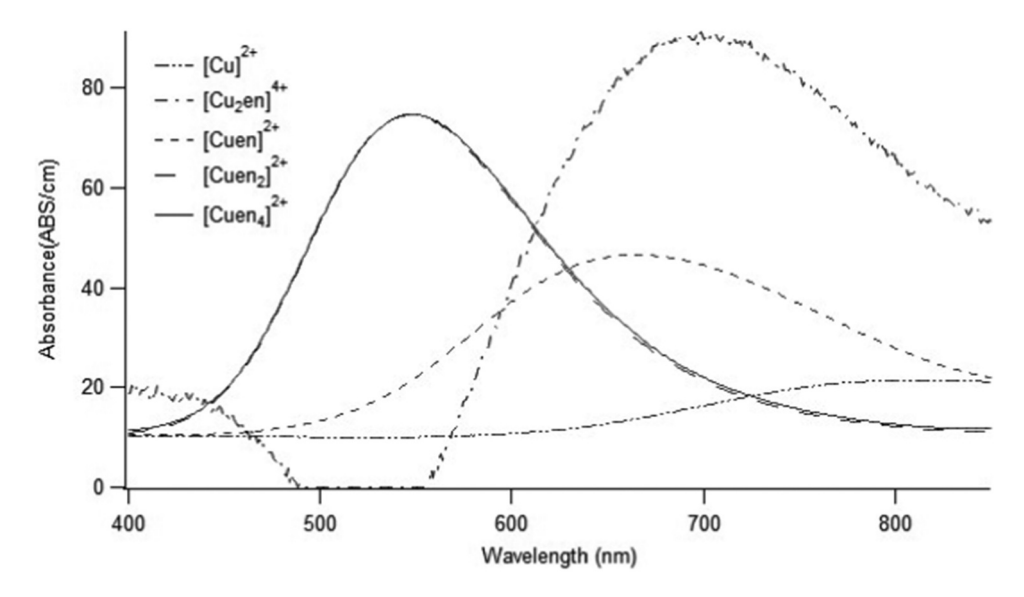


Figure 3. Molar absorptivity curves for the five-factor model fit to DS1.

Table 8. RMSR (restricted and unrestricted) for DS1–5 when fitted to the proposed five-factor model. The Δ signifies the difference between restricted and unrestricted RMSRs. The $\Delta\Delta$ values signify the difference between the two Δ values and indicate the plausibility of the fifth factor.

			4-factor			5-factor	
	4-factor restricted	4-factor unrestricted	RMSR	5-factor restricted	5-factor unrestricted	RMSR	
Dataset	RMSR	RMSR	Δ	RMSR	RMSR	Δ	ΔΔ
DS1	0.000961	0.000178	0.000782	0.000746	0.000172	0.000574	0.000208
DS2	0.001879	0.000777	0.001102	0.001578	0.000738	0.000840	0.000262
DS3	0.001713	0.000271	0.001442	0.001463	0.000239	0.001224	0.000218
DS4	0.002092	0.000483	0.001609	0.001800	0.000413	0.001387	0.000222
DS5	0.001419	0.000824	0.000596	0.001240	0.000774	0.000466	0.000130

Table 9. Binding constants (logK) for the five-factor model with their respective 95% confidence intervals.

Reaction	DS1	DS2	DS3	DS4	DS5
$2[Cu]^{2+} + en \Rightarrow [Cu_2(en-N,N')]^{4+}$	11.63 ^{+0.27} _{+0.02}	$12.00^{+0.45}_{-0.12}$	$12.62^{+0.52}_{-0.13}$	$12.82^{+0.28}_{-0.11}$	11.53 ^{+0.18} _{-0.03}
$[Cu_2(en-N,N')]^{4+}+ en \Rightarrow 2[Cu(en-N,N')]^{2+}$	$9.89^{-0.01}_{-0.16}$	$9.78^{+0.02}_{-0.17}$	$9.12^{+0.03}_{-0.22}$	$9.32^{+0.05}_{-0.11}$	$9.97^{+0.004}_{-0.12}$
$[Cu(en-N,N')]^{2+} + en \Rightarrow [Cu(en-N,N')_2]^{2+}$	$9.20^{+0.02}_{-0.01}$	$9.22^{+0.04}_{-0.02}$	$9.21^{+0.04}_{-0.03}$	$9.28^{+0.03}_{-0.03}$	$9.19^{+0.02}_{-0.005}$
$\frac{1}{2}[Cu(en-N,N')_{2}]^{2+} + en \Rightarrow \frac{1}{2}[Cu(en-N)_{4}]^{2+}$	$6.48^{+0.10}_{-0.54}$	$6.72^{+0.38}_{-0.55}$	$6.84^{+0.33}_{-0.32}$	$6.88^{+0.24}_{-0.22}$	$6.23^{+0.58}_{-0.39}$

Table 10. LogK values for the five-factor model based on all five datasets together. 'Simple Mean' values are the unweighted average of the five logKs from Table 9 with uncertainty ranges of two standard deviations. 'Concatenated datasets' values are generated from fitting all five datasets as a single dataset. 'Common LogKs' values were obtained upon modelling the five datasets simultaneously with the same logK values while allowing the sets of molar absorptivity curves to vary. 'Combined bootstraps' ranges are generated by combining the five bootstrap histograms for each logK and reproducing 95% confidence intervals. 'Best' is the recommended choice, using the mean logKs and the combined bootstraps. Free energy values for the 'best' logK values are also shown in the last column.

Reaction	Simple mean	Concatenated datasets	Common logKs	Combined bootstraps	Best	ΔG° (kJ/mol)
$2[Cu]^{2+} + en \Rightarrow [Cu_2(en-N,N')]^{4+}$	$12.12^{+1.16}_{-1.16}$	10.1 ^{+25.1}	$11.28^{+0.25}_{-0.07}$	11.52 – 13.07	$12.12^{+0.95}_{-0.60}$	-69^{+3}_{-5}
$[Cu_2(en-N,N')]^{4+}+ en \Rightarrow 2[Cu(en-N,N')]^{2+}$	$9.62^{+0.75}_{-0.75}$	$5.4^{+10.9}_{-0.5}$	$8.73^{+0.09}_{-0.13}$	8.95 – 9.97	$9.62^{+0.35}_{-0.67}$	-55^{+4}_{-2}
$[Cu(en-N,N')]^{2+} + en \Rightarrow [Cu(en-N,N')_2]^{2+}$	$9.22^{+0.05}_{-0.05}$	$5.8^{+10.6}_{-0.3}$	$8.36^{+0.09}_{-0.02}$	9.19 – 9.29	$9.22^{+0.07}_{-0.03}$	$-53^{+0.2}_{-0.4}$
$\frac{1}{2}[Cu(en-N,N')_{2}]^{2+} + en \Rightarrow \frac{1}{2}[Cu(en-N)_{4}]^{2+}$	$6.63^{+0.55}_{-0.55}$	$3.0^{+9.9}_{-5.2}$	$5.83^{+0.14}_{-0.09}$	5.87 - 7.13	$6.63^{+0.50}_{-0.76}$	xx
RMSR ($\times 10^3$)	1.473	160.4	1.471	N/A	1.473	1.473

number of molecules in the system. For the five datasets, the maximum amount of the bridging species at half an equivalent of ethylenediamine ranges from 3% to 22%.

The molar absorptivity curves for the five-factor model also parallel those from the four-factor model. The molar absorptivity curve for the bridging species is consistently around 701 nm but is quite noisy because of the low



concentrations that it forms during the titration. They also curiously bottom out in the baseline around 520 nm. This is likely an attempt to correct for something minor in the model around this wavelength early in the titration.

Computational chemistry

The computational thermodynamic values of pertinent species are shown in Table 11. Water molecules were explicitly included as necessary to complete the squareplanar coordination around the copper(II) metal centres. The values are orders of magnitude larger than typical formation energy values, because the reference state is not elements in their standard states. However, the thermodynamic reaction values calculated from them should still represent correctly the sign.

Table 12 depicts how the above computational values were used to confirm the spontaneity of the four-factor model reactions and to calculate the thermodynamic stability of chelate and suprachelate reactions.

Density functional theory generated meaningful, if inaccurate, values for free energy, enthalpy and entropy for the species and reactions discussed in this paper. $[Cu(en-N)_4]^{2+}$ is the complex with the most entropy, while $[Cu(NH_3)_4]^{2+}$ is the complex with the least. More importantly, the computations for the chemical reactions (Table 12) qualitatively match the PERGA results for the four-factor model. The first two reactions that replace two water molecules with an ethylenediamine are all spontaneous ($\Delta G^{\circ} < 0$), enthalpy driven (ΔH° < 0), and entropy driven (ΔS°

Table 11. Thermodynamic values obtained from computational modelling.

Species	ΔG° (kJ/mol)	ΔH° (kJ/mol)	ΔS° (J/mol/K)
en	-500,218	-500,132	287
NH ₃	-148,538	-148,480	192
H ₂ O	-200,697	-200,641	188
$[Cu(H_2O)_4]^{2+}$	-2,396,971	-2,396,885	289
[Cu(NH ₃) ₄] ²⁺	-2,217,273	-2,217,190	279
$[Cu(en-N,N')(H_2O)_2]_2^{2+}$	-2,501,302	-2,501,213	301
$[Cu(en-N,N')(NH_3)_2]^{2+}$	-2,434,271	-2,434,182	298
$[Cu(en-N,N')_2]^{2+}$	-2,648,999	-2,648,906	311
$[Cu(en-N,N')(en-N)_2]^{2+}$	-3,267,900	-3,267,801	333
$[Cu(en-N)_4]^{2+}$	-3,684,690	-3,684,583	360
$[Cu_2(\mu-en-N,N')(H_2O)_6]^{4+}$	-4,911,749	-4,911,646	345

> 0). The third reaction, which brings in two more ethylenediamine ligands, is still spontaneous because it is enthalpy driven, but the entropy change is now negative due to the decrease in the number of free molecules. The fourth reaction, which is used with the five-factor model to make $[Cu_2(\mu-en-N,N')]^{4+}$, was also confirmed to be spontaneous, enthalpically driven.

As expected, these calculations confirm the spontaneity of the chelate effect. The fifth and sixth reactions, which each replace two monodentate ligands with a bidentate ligand, are both enthalpically and entropically driven.

The suprachelate effect, as depicted by the third reaction, highlights the chemistry beyond the chelate effect wherein monodenticity overtakes bidenticity. This occurs late in the titration when the equivalents of ethylenediamine exceed two. Note that this reaction is enthalpically, but not entropically, driven according to the computational results.

Discussion

While single crystal X-ray diffraction may be the ultimate way to characterise a pure compound in chemistry, many interesting species cannot be isolated or crystallised. Being able to characterise ensembles of molecules is exceptionally valuable in supramolecular chemistry.

Modelling full spectra from a spectrophotometric titration is a powerful way to characterise complicated chemical systems at equilibrium. Not only are the number of distinct chemical species able to be determined but also their molar absorptivity curves and the binding constants for the reactions between them. No datum is left out of the modelling process. The various components of the answer reinforce each other as the correct model. This chemometric approach for studying chemistry is an especially effective way to identify non-isolatable species like $[Cu(en-N)_4]^{2+}$.

All five spectrophotometric titrations confirm that copper(II) coordinates stepwise with two ethylenediamine molecules. The logK values match the literature closely, and despite variations in counteranion, spectrometer, experimenter, and environmental condition, the

Table 12. Computation thermodynamic values for reactions involving Cu(II) and en.

	ΔG°_{rxn}			
	Reaction	(kJ/mol)	ΔH°_{rxn} (kJ/mol)	ΔS°_{rxn} (J/mol/K)
1	$[Cu(H_2O)_4]^{2+}$ + en \Rightarrow $[Cu(H_2O)_2(en-N,N')]^{2+}$ + $2H_2O$	-5507	-5477	101
2	$[Cu(en-N,N')]^{2+} + en \Rightarrow [Cu(en-N,N')_2]^{2+} + 2H_2O$	-48872	-48842	98
3	$[Cu(en-N,N')_2]^{2+} + 2en \Rightarrow [Cu(en-N)_4]^{2+}$	-35255	-35412	-885
4	$[Cu(H_2O)_4]^{2+}$ + ½en \Rightarrow ½ $[Cu_2(\mu-en-N,N')(H_2O)_6]^{4+}$ + H_2O	-9492	– 9513	-72
5	$[Cu(NH_3)_4]^{2+}$ + en \Rightarrow $[Cu(en-N,N')(NH_3)_2]^{2+}$ + $2NH_3$	-13856	-13820	116
6	$[Cu(en-N,N')(NH_3)_2]^{2+} + en \Rightarrow [Cu(en-N,N')_2]^{2+} + 2NH_3$	-11586	-11552	110

variance in the fits was remarkably small. The molar absorptivity curves are also entirely as the literature and theory assert. Our data correlate well with previous literature, as no amount of ethylenediamine blueshifted the spectra past the peak location of $[Cu(en-N,N')_2]^{2+}$ (548 nm) nor redshifted it back as would be predicted by the pentaamine effect.

All five titrations support the existence of a fourth species that emerges late in the titration and has a peak absorbance at 548 nm. The evidence discussed herein points to a tetra-coordinated amine/copper(II) complex: either $[Cu(en-N,N')(en-N)_2]^{2+}$ or, more likely, $[Cu(en-N)_4]^{2+}$. Either one involves at least two dangling ethylenediamine ligands. Chemically this is not unreasonable as copper(II) has its preferred square planar coordination and there are plenty of ethylenediamine equivalents around. The chelate effect would suggest that ethylenediamine should coordinate in a bidentate fashion with just two per copper(II) centre; however, given favourable thermodynamics, the system pushes beyond the chelate effect, freeing the second amine on the ethylenediamine ligand to dangle away from the complex.

The surprising existence of $[Cu(en-N)_4]^{2+}$ points to what we label the suprachelate effect, in which chemical assemblies are pushed beyond the chelate effect as thermodynamic forces manifest through dangling ligands. This effect appears to be enthalpically driven, which would suggest that the total amount of H-bonding may be greater when the ethylenediamine ligands dangle - possibly providing better access by water molecules to the coordinated amine.

Several authors discuss effects related to the chelate effect. Kiss et al. identify an 'extra-chelate' effect that is simply a compounded chelate effect wherein three bidentate ligands are linked together to form an especially strong-binding hexadentate ligand [31]. Fanshawe et al. talk about overcoming the chelate effect, but they accomplish this by protonating ethylenediamine ligands and providing only one labile coordination site on the cobalt(III) metal centres [20].

Moufarrej et al. discuss a 'suprachelate effect' to describe the coordination of a tridentate amine upon deprotonation that leads to the creation of a larger macrocycle [7]. As Ercolani has shown that entropy does lead to the preference of smaller discrete rings over larger ones, he likely would refer to their scheme as chelate cooperativity [32].

Therefore, $[Cu(en-N)_4]^{2+}$ exemplifies the suprachelate effect, as we posit herein. The dangling amines are poised to coordinate to a second metal centre, forming a bridge between multiple Cu(II) centres. Such an assemblage has not yet been reported in the solution phase.

The five-factor model for our titrations points to [Cu₂(µen-N,N')⁴⁺, as the bridging species appears to be the most supported by the data. Bridging of metal centres by ethylenediamine has been studied and observed before, and the suprachelate effect led to ethylenediamine bridging nickel(II) centres in solution [5]. Thus, the suprachelate effect can be harnessed to promote bridging by multidentate ligands. We hope to take advantage of it to synthesise supramolecular squares with copper(II) in aqueous solution.

Acknowledgments

Funding: This work is supported by the National Science Foundation through an RUI grant from the Division of Chemistry (2004005) and an MRI grant (1726260) for the supercomputer (borg.calvin.edu), which supported the computational aspects of this project. We are also grateful to the Arnold and Mabel Beckman Foundation for supporting Calvin University and F.L. as a Beckman Scholar, and the STEAM Ahead program of the state of Michigan for supporting A.E.B. and A.S.

Disclosure statement

No potential conflict of interest was reported by the author(s).

Funding

The work was supported by the Arnold and Mabel Beckman Foundation [Beckman Scholars Program]; Michigan Economic Development Corporation [STEAM Ahead]; Directorate for Mathematical and Physical Sciences (MPS) [2004005].

Supporting information

The supporting information includes export files that can be uploaded and examined at Sivvu.org. Each file contains a spectrophotometric titration dataset along with its final optimised model. There are also text files containing summary information on all data fittings (3/4/5-factor models).

References

- [1] Miessler G; Fischer P; Tarr D. Inorganic chemistry. 5th ed. Boston: Pearson; 2013.
- [2] Rodgers GE. Introduction to coordination, solid-state, and descriptive inorganic chemistry. New York: McGraw-Hill; 1994. p. 128.
- [3] Cotton FA; Wilkinson G; Murillo CA; Bochmann M. Advanced inorganic chemistry. 6th ed. (NY): Wiley-Interscience: 1999.
- [4] Housecroft CE and Sharpe AG. Inorganic chemistry. 2nd ed. New Jersey: Pearson Education; 2005.
- [5] Lawler, F.; Storteboom, R.; Rosales-Lopez, P.; Hoogstra, M.; Selvaggio, K.; Chen, T.; Zogg, K.; Heule, D.; Pehrson, N.J.; Baker, A.E. and Vander Griend, D.A. On the

- - replicability of the thermodynamic modeling of spectroscopic titration data in the nickel(ii) ethylenediamine system. J Chemom. 2024, submitted.
- [6] Chesman ASR; Turner DR; Deacon GB; Batten SR. Metalpromoted nucleophilic addition and cyclization of dicyanonitrosomethanide, Diamines with $[C(CN)_2(NO)]^-$. Chem - An Asian J. **2009**;4(5):761–769. doi: 10.1002/asia.200800323
- [7] Moufarrej T; Bui K; Zompa LJ. Nickel(ii) complexation by Bis(1,4,7-triazacyclononane) ligands with Polymethylene Linker Groups.: a study of the stability and structure of their mononuclear and binuclear dimeric complexes. Inorganica (Rome) Acta. 2002;340:56-64. doi: 10.1016/ 50020-1693(02)01014-9
- [8] Zhang D, Zhang L, Zhao Z, et al. Cyanide-bridged trinuclear and ethylenediamine-bridged one-dimensional Cobalt(III)-Manganese(II) complexes: synthesis, crystal structures and magnetic properties. Bull Korean Chem Soc. 2011;32(8):2544-2548. doi: 10.5012/bkcs.2011.32.8.
- [9] Putaj P; Gaweł B; Łasocha W. Ethylenediamine as a bridging ligand: structure solution of two Cadmium(II)-based coordination polymers from powder diffraction data. Powder Diff. 2013;28(3):207-211. doi: 10.1017/S0885715613000146
- [10] Griffith WP; McManus NT; Skapski AC. X-Ray crystal structure of [Ru₂N(Ethylenediamine)₅]Cl₅.H₂O; a novel complex containing both nitrido and ethylenediamine bridges. J Chem Soc Chem Commun. 1984;(7):434-435. doi: 10.1039/c39840000434
- [11] Sharma J, Jiang Z, Bhutani A, et al. A unique copper coordination structure with both mono- and Bi-dentate ethylenediamine ligands. CrystEngcomm. 2019;21 (17):2718-2726. doi: 10.1039/C8CE02188K
- [12] Inada Y; Ozutsumi K; Funahashi S; Soyama S; Kawashima T: Tanaka M. Structure of Copper(II) ethylenediamine complexes in aqueous and neat ethylenediamine solutions and solvent-exchange kinetics of the Copper(II) ion in ethylenediamine as studied by EXAFS and NMR methods. Inorg Chem. **1993**;32 (14):3010-3014. doi: 10.1021/ic00066a009
- [13] Hathaway BJ; Tomlinson AAG. Copper(ii) ammonia complexes. Coord Chem Rev. 1970;5(1):1-43. doi: 10. 1016/S0010-8545(00)80073-9
- [14] Chattopadhyay S, Bocelli G, Cantoni A, et al. A novel Copper(II) complex with a pendant Schiff base: an unprecedented monodentate bonding mode of the potentially tridentate ligand. Inorganica (Rome) Acta. **2006**;359(13):4441–4446. doi: 10.1016/j.ica.2006.06.009
- [15] Vander Griend DA; Bediako DK; DeVries MJ; DeJong NA; Heeringa LP. Detailed spectroscopic, thermodynamic, and kinetic characterization of Nickel(II) complexes with 2,2'-bipyridine and 1,10-phenanthroline attained via equilibrium-restricted factor analysis. Inorg Chem. 2008;47(2):656-662. doi: 10.1021/ic700553d
- [16] Vander Griend DA; Vermeer M; Kim Y; Greeley M; Buist D; Ulry C; Lee A. SIVVU. sivvu.org/. [cited 2024 Jun 30].
- [17] Thordarson P. Determining association constants from titration experiments in supramolecular chemistry. Chem Soc Rev. **2011**;40(3):1305–1323. doi: 10.1039/C0CS00062K
- [18] Gampp H; Maeder M; Meyer CJ; Zuberbühler AD. Calculation of equilibrium constants from

- multiwavelength spectroscopic data-i: mathematical considerations. Talanta. 1985;32(2):95-101. doi: 10.1016/0039-9140(85)80035-7
- [19] Kazmierczak NP, Vander Griend DA. Properly handling negative values in the calculation of binding constants by physicochemical modeling of spectroscopic titration data. J Chemom. 2019;33(11):3183-3196. doi: 10.1002/ cem.3183
- [20] Fanshawe RL; Mobinikhaledi A; Clark CR; Blackman* AG. Overcoming the chelate effect: hypodentate coordination of ethylenediamine, Diethylenetriamine and Tris(2--Aminoethyl)Amine in Co(III) complexes. Inorganica (Rome) Acta. 2000;307(1):27-32. doi: 10.1016/S0020-1693(00)00184-5
- [21] [cited 2024 Jun 17]. Available from: www.chem.tamu. edu/rgroup/gladysz/Research%20Safety%20Resources/ Perchlorate%20hazards.pdf
- [22] DeSa RJ, Matheson IBC. A practical approach to interpretation of singular value decomposition results. Meth Enzymol. **2004**;384:1–8. doi: 10.1016/S0076-6879(04) 84001-1
- [23] Kazmierczak NP, Chew JA, Vander Griend DA. Bootstrap methods for quantifying the uncertainty of binding constants in the hard modeling of spectrophotometric titration data. Analytica Chimica Acta. 2022;1227:339834. doi: 10.1016/j.aca.2022.339834
- [24] Bjerrum J. Metal ammine formation in aqueous solution. 1941 a complete review is given in C. A. Sft. Copenhagen: P. Haase. 1941. p. 6527-6634.
- [25] Cooper D; Plane RA. Cyanide complexes of copper with ammonia and Ethylenediamine. Inorg Chem. 1966:5 (10):1677-1682. doi: 10.1021/ic50044a009
- [26] Johnson ML. Evaluation and propagation of confidence intervals in nonlinear, asymmetrical variance spaces. Analysis of ligand-binding data. Biophys J. 1983;44 (1):101-106. doi: 10.1016/S0006-3495(83)84281-7
- [27] Carlson GA, McReynolds JP, Verhoek FH. Equilibrium constants for the formation of ammine complexes with certain metallic lons1. J Am Chem Soc. 1945;67 (8):1334-1339, doi: 10.1021/ia01224a036
- [28] Basolo F, Murmann RK. Steric effects and the stability of complex compounds. I. The chelating tendencies of N-Alkylethylenediamines, with Copper(II) and Nickel(II) lons1. J Am Chem Soc. 1952;74(21):5243-5246. doi: 10. 1021/ja01141a002
- [29] Yogi DS, Venkataiah P, Mohan MS, et al. Equilibrium studies on ternary Cu(II) complexes containing adenosine-5'-triphosphate. Indian J Chem. 1994;33A (4):407-411. doi: 10.1007/BF02843276
- [30] Silva JA, Felcman J, Merce LR, Mangrich AS, Lopes RSC, Lopes CC. Study of binary and ternary complexes of copper(ii) with some polyamines and adenosine 5' triphosphate. Inorg Chim Acta. 2003;356:155-166. doi: 10. 1016/S0020-1693(03)00462-6
- [31] Kiss T; Farkas E. Metal-binding ability of desferrioxamine B. J Inclusion Phenom. 1998;32(2):385-403. doi: 10. 1023/A:1008046330815
- [32] Ercolani G; Schiaffino L. Allosteric, Chelate, and Interannular Cooperativity: a mise Au point. Angew Chem Int Ed. 2011;50(8):1762-1768. doi: 10.1002/anie. 201004201